

Ozone concentration simulations considering light intensity of BVOC emissions

Akira Kondo¹, Sho Hashimoto¹, Hikari Shimadera¹, Yoshio Inoue¹

¹Osaka University

²Osaka University

³Osaka University

⁴Osaka University

kondo@see.eng.osaka-u.ac.jp

hashimoto@ea.see.eng.osaka-u.ac.jp

shimadera@ea.see.eng.osaka-u.ac.jp

inoue@see.eng.osaka-u.ac.jp

Abstract. Monoterpene emissions from coniferous trees in Japan depend on light intensity as well as temperature. The light intensity of monoterpene emissions were evaluated by the growth chamber experiment and the empirical equation on the light intensity of monoterpene emissions was proposed. Ozone concentrations in the Kinki region of Japan during one month of July 2008 were calculated by using WRF/CMAC with two types of different BVOC emissions. It was suggested that the increase of monoterpene emissions at daytime decreased the maximum ozone concentration level, and the decrease of emissions at nighttime raised the minimum ozone concentration level. The difference of monoterpene emissions due to light intensity affected ozone concentration relatively greatly.

Keywords: monoterpene, light intensity, ozone, WRF/CMAQ

1. Introduction

Photochemical oxidants cause a lot of damage to humans and vegetation. The increase in precursor emissions (oxides of nitrogen and volatile organic compounds) of ozone can significantly increase the ozone pollution. It is well known that biogenic volatile organic compound (BVOC) emission increases with the rise in temperature and that BVOC plays an important role in the generation of ozone. Though the impact of biogenic emission on ozone pollution is mainly observed in rural and suburban sites (Tsigaridis and Kanakidou, 2002), it can also be significant in urban region (Solmon et al., 2004). In Japan, the standard for the photochemical oxidant was formulated in 1970, and due to its effectiveness, the concentration of photochemical oxidant decreased until 1990. However, recently the concentration of photochemical oxidant has been gradually increasing in Japan. One of its causes is the increase of the background ozone concentration due to transboundary transport (Akimoto, 2003). Furthermore, temperature increase due to global warming, urban heat island and the increase of ultraviolet rays (Wakamatsu et al., 1996) are also considered as some of its major causes. Vogel et al. (1995) reported that simulations without using biogenic VOC emissions show a maximum difference in the ozone concentration of 18 ppb. Solmon et al. (2004) found that, when biogenic emission was included in the simulation, the simulated surface ozone concentration reached 18-30% in Paris. Bao et al. (2009) reported that biogenic emission made the average ozone concentration rise of 5ppb in the Kinki region in Japan. The leaf temperature dependency of the monoterpene which is a kind of BVOC emissions from coniferous trees is known well. This study showed that monoterpene emissions depended on light intensity as well as leaf temperature, and estimated the impact on ozone concentrations due to light intensity dependency of monoterpene by using WRF/CMAQ.

2. Growth chamber experiment

Three coniferous trees (*P. densiflora*, *C. obtuse* and *C. japonica*) were selected to measure monoterpene emissions because they were the dominant coniferous trees in the Kinki region, Japan. Nine kind of monoterpene (α -Pinene, β -Pinene, β -Myrcenem, α -Phellandrene, α -Terpinene, p-Cymene, Limonene, γ -Terpinene, and Terpinolene) were analyzed. The outline

of the growth chamber experiment is shown in Fig.1. The six plants planted in 10 l plastic pots were placed into the growth chamber before a day of the experiment. Air samples of 6 l were collected by Tenax-TA adsorbent tube connected to a vacuum pump (GL Science SP208-1000Dual) with a flow rate of 100 ml/min at every 3 h. The trapped compounds in the adsorbent tubes were analyzed by GC/MS (Shimadzu GC/MS-QP2010) equipped with Thermal Desorber (Perkin Elmer ATD-50). The experiments were conducted for varying PAR (Photosynthetically Active Radiation) of 0, 500, 700, 850, 1200, and 1400 [$\mu\text{mol m}^{-2}\text{s}^{-1}$]. Though air temperature in the growth chamber was kept at the constant of 30°C, leaf temperature slightly rose for light intensity. Tingey (1981) proposed the equation of monoterpene emissions.

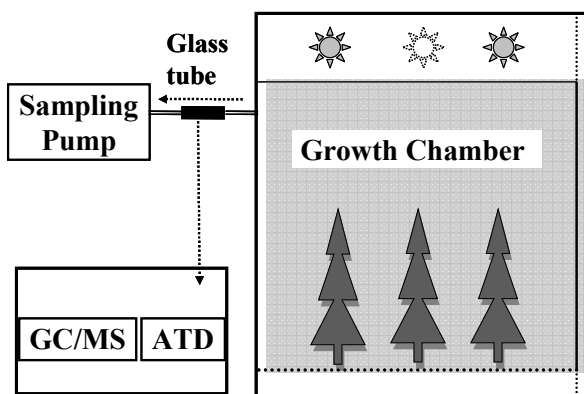


Fig.1 Outline of growth chamber experiment

$$M = M_S \exp(\beta(T - T_S)) \quad (1)$$

where, M_S [$\mu\text{g g}_{\text{dw}}^{-1}\text{h}^{-1}$] is monoterpene emission at the standard temperature T_S [303K] and β is the empirical coefficient which varies at the range of 0.057-0.144 [K^{-1}] for the kind of trees. But the values of 0.09 [K^{-1}] was commonly used. The experimental values were corrected by the Eq.(1) of $\beta = 0.09$. In growth chamber experiment, monoterpene concentration decreases due to the deposition on the surface and due to the decomposition. In order to consider the correction of monoterpene concentration due to these Influences, the decay experiment was conducted for all kind of monoterpene.

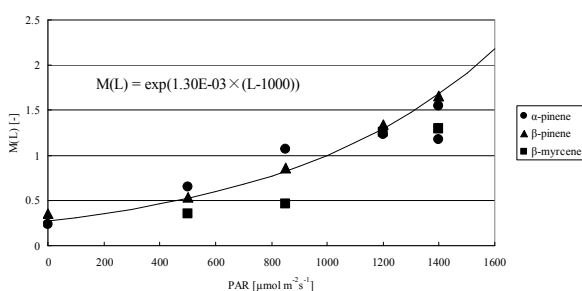


Fig.2 The light intensity *P. densiflora*

The equation of monoterpene emissions considering light intensity as well as leaf temperature was proposed by

$$M = M_S \exp(\beta(T - T_S)) \exp(\gamma(L - L_S)) \quad (2)$$

where, M_S [$\mu\text{g g}_{\text{dw}}^{-1}\text{h}^{-1}$] is monoterpene emission at the standard temperature T_S [303K] at the standard light intensity L_S [$1000 \mu\text{mol m}^{-2}\text{s}^{-1}$] and γ is the empirical coefficient. The relation of light intensity and of $M(L)$ for α -Pinene, β -Pinene, and β -Myrcenem emitted from *P. densiflora* are shown in Fig.2. $M(L)$ is $\exp(\gamma(L - L_S))$ of Eq.(2). From the experiment, γ of 1.3×10^{-3} was estimated. The relation of light intensity and of $M(L)$ for α -Pinene, β -Pinene, and Limonene emitted from *C. obtuse* are shown in Fig.3. From the experiment, γ of 7.35×10^{-4} was estimated. The relation of

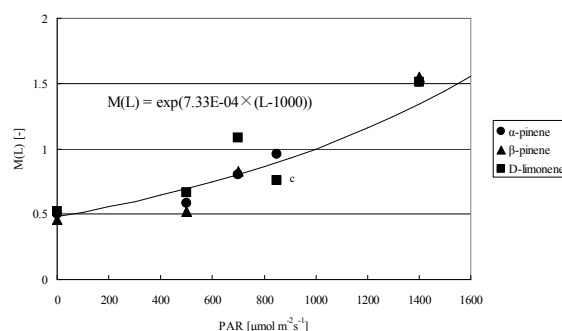


Fig.3 The light intensity *C. obtuse*

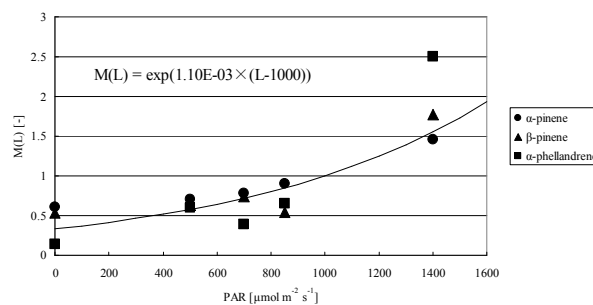


Fig.4 The light intensity *C. japonica*

light intensity and of $M(L)$ for α -Pinene, β -Pinene, and α -Phellandrene emitted from *C. japonica* are shown in Fig.4. From the experiment, γ of 1.10×10^{-3} was estimated. There wasn't the great difference of γ among three coniferous trees. Therefore the common value of γ was determined. Considering the light intensity, with which the photosynthetic rate is saturated, the equation (2) was rewrite by

$$\begin{aligned} M &= M_s \exp(\beta(T - T_s)) \exp(1.04 \times 10^{-3}(L - L_s)) & L \leq 1600 \\ M &= M_s \exp(\beta(T - T_s)) \exp(1.04 \times 10^{-3}(1600 - L_s)) & L \geq 1600 \end{aligned} \quad (3)$$

3. WRF/CMAQ outline

In order to simulate ozone concentration, WRF (Weather Research and Forecasting model) and CMAQ (Community Multiscale Air Quality modeling system) were used. The calculation conditions of WRF and of CMAQ used were summarized in Table 1.

Table 1 The calculation conditions of WRF and of CMAQ

Parameter	Setting
Spin-up period	24 - 30 June 2008
Simulation period	July 2008
Output interval	1 hour
Map projection	Lambert conformal conic
Central point	32.5° N, 125° E
Horizontal grid spacing	64, 16 and 4 km
Vertical domain	24 layers (Ground surface - 100 hPa)
WRF	
Version	ARW 3.2.1
Horizontal grid number	120 × 108, 84 × 84 and 84 × 84
Initial and boundary	NCEP.FNL and GPV-MSM
Analysis nudging	$G_{t, q, uv} = 5.0^{-5} \text{ s}^{-1}$ in D1 and D2
Explicit moisture	WSM3
Cumulus	Kain-Fritsch
PBL and surface layer	YSU PBL and Monin-Obukhov similarity
Surface	Noah LSM
Radiation	RRTM and Goddard
CMAQ	
Version	4.7.1
MCIP	Version 3.6
Horizontal grid number	108 × 96, 72 × 72 and 72 × 72
Initial and boundary	CMAQ default concentration profile
Advection	Yamartino scheme
Horizontal diffusion	Multiscale
Vertical diffusion	ACM 2
Photolysis calculation	JPROC table
Gas phase chemistry	SAPRC-99
Chemistry solver	EBI
Aerosol	AERO5
Cloud and aqueous chemistry	On

The WRF/CMAQ modeling system was applied to the Kinki Region of Japan in July 2008. Fig. 5 shows the modeling domains consisted of 3 domains from domain 1 (D1) covering a wide area of East Asia to domain 3 (D3) covering most of the Kinki Region. The horizontal resolutions in the domains are 64, 16 and 4 km, respectively. The vertical layers consist of 24 sigma-pressure coordinated layers from the surface to 100 hPa with approximately 15, 50 and 110 m as the middle height of the first, second and third layer, respectively.

Emission data applied in this study include anthropogenic, biogenic VOCs (BVOCs) biomass burning and volcanic SO₂ emissions. Anthropogenic for the Japan region were derived from EAGrid2000-Japan (Kannari et al., 2007). In Japan, air pollution in roadside areas has been improving since the Law concerning Special Measures for Total Emission Reduction of Nitrogen Oxides and Particulate Matter from Automobiles in Specified Areas (Automobile NO_x/PM Law) was enacted in 2001. To reflect the situation, vehicles' exhaust emissions in EAGrid2000-Japan were cut according to decreasing rates of air pollutant concentrations observed at the roadside air pollution monitoring stations in Hyogo Prefecture. BVOCs emissions were estimated according to Bao et al.(2009). In addition, light intensity of monoterpene emissions was considered For the other Asian countries, anthropogenic emissions of SO₂, NO_x, CO, VOCs and PM were obtained from an emissions inventory for Asia in the year 2006 developed to support the Intercontinental Chemical Transport Experiment-Phase B (INTEX-B) (Zhang et al., 2009). Emissions of NH₃ were derived from predicted values for the year 2005 in regional emission inventory in Asia (REAS) (Ohara et al., 2007). BVOCs and biomass burning emissions were derived from Murano (2006) and Streets et al. (2003), respectively. The volcanic SO₂ emission fluxes were obtained from Andres and Kasgnoc (1998) for volcanoes erupting SO₂ continuously, and observation data by JMA for Miyakejima located to the south of Tokyo. The standard monoterpene emission map in the Kinki region is shown in Fig.6.

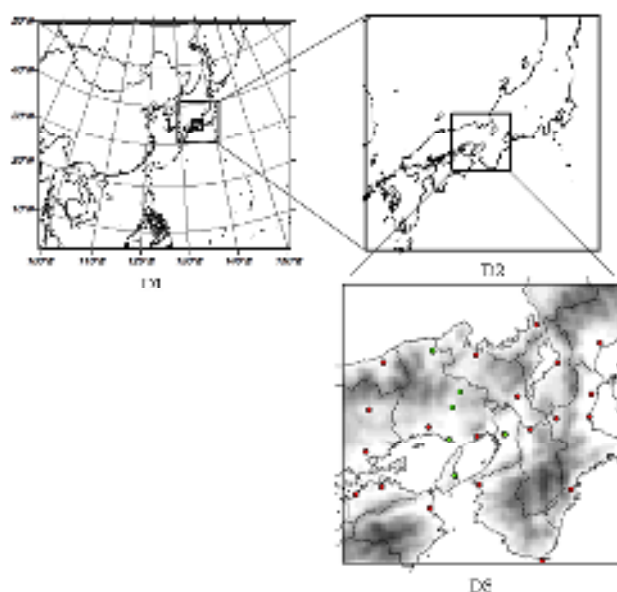


Fig.5 The calculated domain

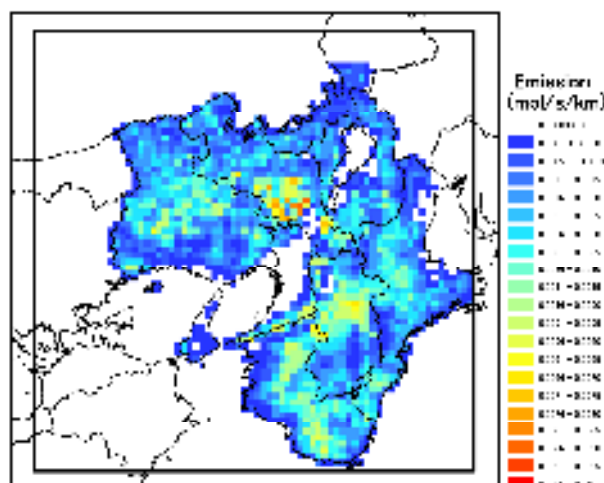


Fig.6 The standard monoterpene emission map in the Kinki region

4. Results

- Table 2 The statistical values

	Height	MBE	MAE	IA
Temperature	2m	≤ ±2.0°C	≤ 2.1°C	≥ 0.73
Humidity	2m	≤ ±2.6 g kg ⁻¹	≤ 2.6 g kg ⁻¹	≥ 0.56
Wind speed	10m	≤ ±2.8 m s ⁻¹	≤ 3.5 m s ⁻¹	≥ 0.33
Ozone		≤ 15.1 ppb	≤ 16.4 ppb	≥ 0.67

WRF results were compared with data at 24 meteorological observatories represented in red circle of D3. The statistical indicators of Correlation Coefficient, Mean Bias Error, Mean Absolute Error, Root Mean Square Error, and Index of Agreement were used in order to verify the accuracy of WRF results. The statistical values were summarized in Table 2. WRF well represented temperature and humidity but there are some problems regarding the representation of wind speed.

Ozone concentrations were simulated by CMAQ against two different monoterpene emission data. One was the emission data depended at only temperature (case1) and another was the

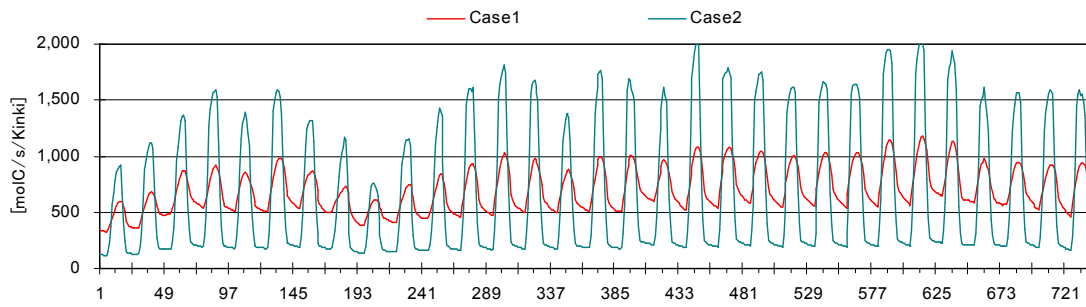


Fig.7 The hourly variation of monoterpene emission in case1 and in case2

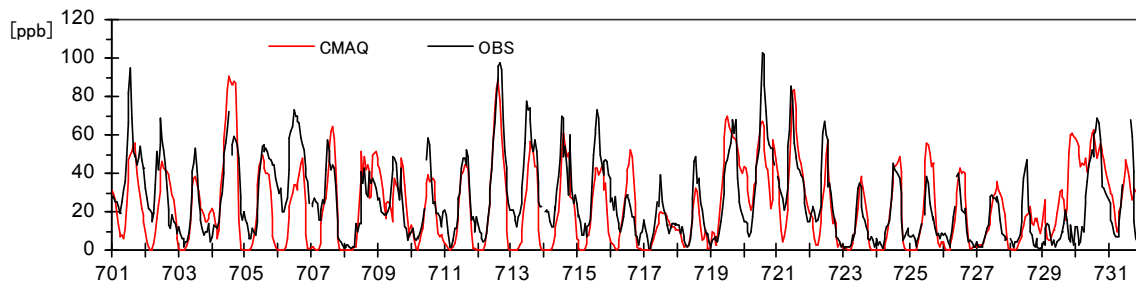


Fig.8 The hourly variation of the simulated and the observed ozone concentration at Osaka

emission data depended at both temperature and light intensity (case2). Figure 7 shows the hourly variation of monoterpene emission in case1 and in case2. The diurnal amplitude in case2 was larger than in case1. The monoterpene emission in case1 and case2 was 5.16×10^5 [molC s⁻¹] and 4.90×10^5 [molC s⁻¹], respectively. The simulated ozone concentrations were compared with data at 6 observatories represented in green circle of D3. The statistical values in case1 were summarized in Table 2. There were no significant differences between case1 and case2. CMAQ well represented ozone concentration. The hourly variation of the simulated and the observed ozone concentration at Osaka is shown in Fig.8. The monthly average ozone concentration in the Kinki region is shown in Fig.9 and the difference of the monthly average ozone concentration in the Kinki region between case1 and case2 is shown in Fig.10. It was found that ozone concentration increased in the forest area and decreased in the urban area.

The difference of the hourly average ozone concentration at 0JST and 7JST between case1 and case2 is shown in Fig.11. The average difference of ozone concentration was -0.031ppb.

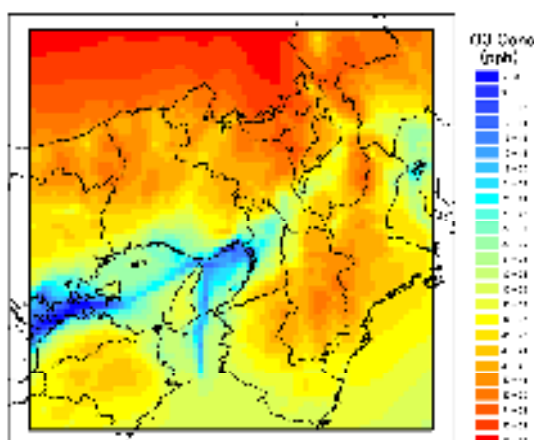


Fig.9 The monthly average ozone concentration in the Kinki region

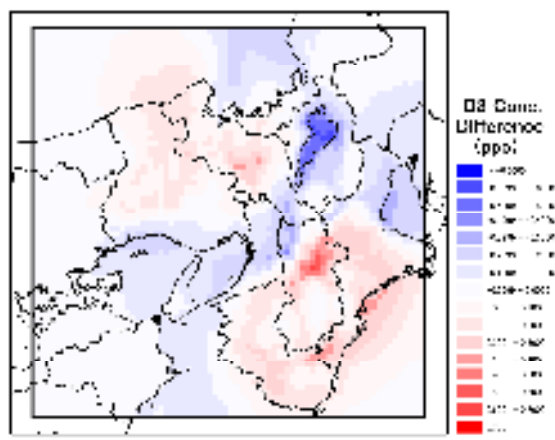


Fig.10 the difference of the monthly average ozone concentration in the Kinki region between case1 and case2

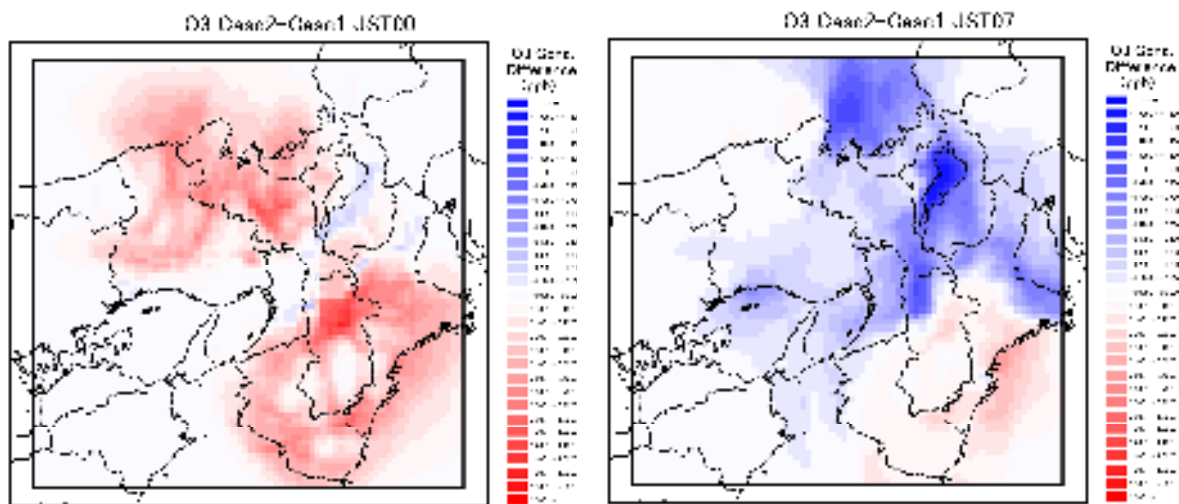


Fig.11 The difference of the hourly average ozone concentration at 0JST and 7JST between case1 and case2

The maximum difference in nighttime and the minimum difference in daytime were 1.8ppb and -2.7ppb, respectively. The difference of monoterpene emissions due to light intensity affected ozone concentration relatively greatly.

References

- Andres, R.J., Kasgnoc, A.D., A time-averaged inventory of subaerial volcanicsulfur emissions. *Journal of Geophysical Research D: Atmospheres* 103 (D19),25251–25261,1998.
- Akimoto, H., Global air quality and pollution. *Science* 302 (5651), 1716-1719, 2003.
- Hai Bao. Et al., Modeling the influence of biogenic volatile organic compound emissions on ozone concentration during summer season in the Kinki region of Japan , *Amspheric Environment* , 421-431, 2009.
- Kannari A., Tonooka Y., Baba T., Murano K., Development of multiple-species 1 km × 1 km resolution hourly basis emissions inventory for Japan. *Atmospheric Environment*, 41(16), 3428-3439, 2007.
- Murano, K., International Co-operative Survey to Clarify the Trans-boundary Air Pollution Across the Northern Hemisphere (Abstract of the Final Report). Summary Report of Research Results under the GERP (Global Environment Research Fund) in FY2004, pp. 237–243, Research and Information Office, Global, Environment Bureau, Ministry of the Environment, Government of Japan, 2006..
- Ohara, T., Akimoto, H., Kurokawa, J., Horii, N., Yamaji, K., Yan, X., Hayasaka, T., An Asian emission inventory of anthropogenic emission sources for the period1980–2020. *Atmospheric Chemistry and Physics* 7 (16), 4419–4444, 2007..
- Solmon, F., Sarrat, C., Sercxa, D., Tulet, P., Rosset, R., Isoprene and monoterpenes biogenic emissions in France: modeling and impact during a regional pollution episode. *Atmospheric Environment* 38 (23), 3853-3865, 2004.
- Streets D.G., Yarber K.F., Woo J.-H., Carmichael G.R., Biomass burning in Asia: Annual and seasonal estimates and atmospheric emissions. *Global Biogeochemical Cycles*, 17(4), 10/1-10/20, 2003.
- Tingey, D.T., et al., Influence of light and temperature on monoterpene emission rates from slash pine. *Plant Physiology* 65 (5), 797-801, 1980.
- Tsigaridis, K., Kanakidou, M., Importance of volatile organic compounds photochemistry over a forested area in central Greece. *Atmospheric Environment* 36 (19), 3137-3146, 2002.
- Vogel, B., Fiedler, F., Vogel, H., Influence of topography and biogenic volatile organic compounds emission in the state of Baden-W€urttemberg on ozone concentrations during episodes of high air temperatures. *Journal of Geophysical Research* 100 (D11), 22907-22928, 1995.
- Wakamatsu, S., Ohara, T., Uno, I., Recent trends in precursor concentrations and oxidant distributions in the Tokyo and Osaka areas. *Atmospheric Environment* 30 (5), 715-721, 1996.
- Zhang Q., et al., Asian emissions in 2006 for the NASA INTEX-B mission. *Atmospheric Chemistry and Physics Discussions*, 9(1), 4081-4139, 2009.